THE JOURNAL OF PHYSICAL CHEMISTRY A

 VOLUME 105, NUMBER 28, JULY 19, 2001

ARTICLES

Photodissociation Dynamics of Acetic Acid and Trifluoroacetic Acid at 193 nm

Hyuk Tae Kwon, Seung Keun Shin, Sang Kyu Kim,† and Hong Lae Kim*

Department of Chemistry, Kangwon National University, Chuncheon 200-701, Korea

Chan Ryang Park

Department of Chemistry, College of Natural Sciences, Kookmin University, Seoul 136-702, Korea

Received: February 28, 2001; In Final Form: May 2, 2001

Photodissociation dynamics of acetic acid and trifluoroacetic acid at 193 nm have been investigated by measuring laser-induced fluorescence spectra of OH fragments. The OH fragments are produced exclusively in the ground electronic state. The measured energy distributions among the fragments are $f_t(OH) = 0.05$, $f_t = 0.42$, $f_{int}(Ac) = 0.53$ and $f_t(OH) = 0.05$, $f_t = 0.33$, and $f_{int}(FAc) = 0.62$, for acetic and trifluoroacetic acid, respectively, and negligible vibrational excitation in the OH fragments was observed. The dissociation does not depend on the polarization of the dissociating light. It was concluded from the measured energy distribution and no polarization dependence that the electronic transition at 193 nm leads the parent molecule to the singlet excited surface, and the dissociation takes place along the triplet surface with an exit channel barrier. From the estimated internal energies in the acetyl radicals, the lifetimes of the acetyl radicals are estimated from the RRKM theory.

Introduction

Studies on photodissociation of carbonyl compounds such as acetone in UV have been reported extensively.[1−4] Absorption centered at around 260 nm is assigned as $n \rightarrow \pi^*$, which produce acetyl radicals as major products with the quantum yield of near unity. On the other hand, at shorter wavelengths, the $n \rightarrow 3s$ Rydberg transition breaks two C−C bonds in acetone, producing two methyl radicals and CO as fragments. Previous studies on the dissociation of these compounds were concentrated on mechanisms to determine whether this three-body dissociation takes place via a concerted or stepwise manner. The very recent study on acetone by the femtosecond pump−probe technique demonstrated that dissociation occurs in a stepwise manner when the photon energy is large enough to break both C−C bonds.[5] The measured lifetime of the acetyl radical is around 500 fs and the dissociation dynamics of the acetyl radical is successfully modeled by the RRKM theory. Since the dissociation rates depend exponentially on the energy of the acetyl radicals, the internal energies should be measured precisely in order to estimate the lifetimes of the acetyl radicals.

Studies of molecular photodissociation dynamics are of fundamental importance to investigate electronic structures of molecules because the process is governed by the excited state and potential energy surfaces along the reaction coordinate. The detailed dynamics of the process can be understood by measuring energies and certain vector properties of the system. These physical properties of the system can be measured precisely from optical spectra in favorable cases where the photofragments absorb and/or emit radiation in an easily accessible spectral region. The Doppler broadened absorption or emission spectra of the photofragments by polarized photolysis and probe light provide information on the energy distribution among various

* Corresponding author e-mail: hlkim@cc.kangwon.ac.kr
† Department of Chemistry, Inha University, Inchon 402-751, Korea.

10.1021/jp010787v CCC: $20.00
Published on Web 06/22/2001

degrees of freedom of the fragments as well as directions of the transition dipole moment, recoil velocity, and angular momenta of the fragments. From the measurements, the excited state and the potential energy surfaces along the reaction coordinate can be identified.

Photodissociation dynamics of acetic acid by irradiation of UV light have been reported for many years.[6−10] The lowest $n \rightarrow \pi^*$ transition produces the OH and acetyl radicals as major products. At 200 and 218 nm, the energy distributions were measured from the photodissociation of acetic acid, from which the indirect dissociation via curve crossing with a reverse barrier was suggested.[7,8] Recently, the lifetimes of the acetic acid and the acetyl radical from the photodissociation of acetic acid at 194.5 nm were measured to be 200 fs and 5 ps, respectively, from the femtosecond pump−probe technique.[11] The lifetime of the acetyl radical was successfully estimated by the statistical RRKM theory. However, the internal energy was assumed from the linear disposal of the available energy into the internal energy of the products based upon the previous 200 and 218 nm photodissociation studies. However, to model the dissociation dynamics of the acetyl radicals, the internal energy should directly be measured.

In the present study, the photodissociation dynamics of acetic acid and trifluoroacetic acid have been investigated by measuring the laser induced fluorescence spectra of the OH fragments. From the spectra, the complete energy distribution has been deduced and lifetimes of the acetyl and trifluoroacetyl radicals were estimated from the measured average internal energies in the radical products.

Experiment

The experiment was performed in a flow cell with conventional pump−probe geometry. The cell is a cube made of stainless steel with four arms in which baffles are placed to minimize scattered light. The cell was evacuated at a pressure of about 10^{-3} Torr and the gaseous sample was continuously flowed at a sample pressure of about 50 mTorr. The acetic acid and trifluoroacetic acid, purchased from Aldrich (99% purity), were used without further purification.

The 193 nm dissociating light was obtained from an ArF excimer laser (Lambda Physik Lextra 50), whose output was linearly polarized with a stack of quartz plates at a Brewster angle. The horizontally polarized probe light was a frequency-doubled output of a dye laser (Lumonics HD-500) pumped by the second harmonic of an Nd:YAG laser (Lumonics YM-800). The two laser beams were temporally separated by about 50 ns. The 50 ns delay time between the pump and probe light and 50 mTorr sample pressure should ensure nascent product energy distribution. The laser induced fluorescence (LIF) spectra of the OH fragments were measured employing the A−X transition in UV. The 0−0 transition of OH was excited and the resulting total fluorescence was probed through a filter (UG-11). The power of the probe laser light was kept as low as possible (typically 20 μJ/pulse) to avoid saturation and to minimize the scattered radiation. The scattered radiation was also cut off through baffles, which are placed in the arms attached to the cell. The laser-induced fluorescence was detected through a collection lens by a PMT (Hamamatsu R212UH) whose direction of view was at a right angle to the two laser beams, and the detected signal was fed to a boxcar averager. The powers of the dissociating and the probe lights were measured separately, and the detected signal was corrected for variation of the laser powers. A signal processor digitized the signal that was stored and processed in a PC.

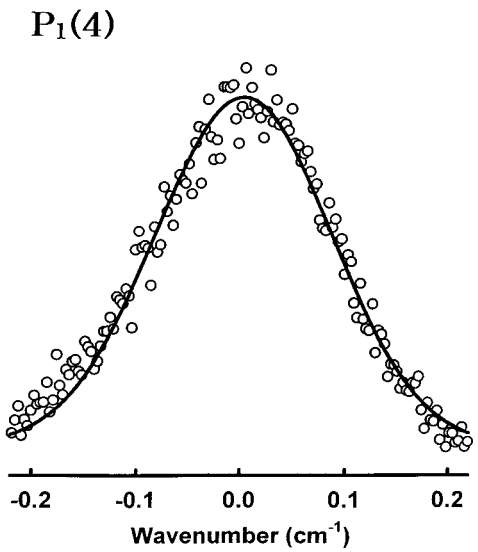

Figure 1. Rotationally resolved LIF spectrum of OH produced from the photodissociation of acetic acid at 193 nm. The $P_1(4)$ rotational transition in the 0−0, A←X transition is shown at the 20 mTorr sample pressure, 5 Torr He, and 5 μs pump−probe delay time for collisional speed relaxation.

The bandwidth of the probe laser light is 0.08 cm^{-1} in the visible that was measured by the line width of the rotationally resolved OH LIF spectra obtained by photodissociation of the sample after collisional relaxation by about 5 Torr of He at long pump−probe delay time (Figure 1). The horizontally polarized dissociating and probe laser beams were collinearly counter-propagated or introduced at a right angle to the cell to obtain two different experimental geometries. The Doppler profiles of the spectra for several rotational transitions were probed in order to search for the polarization dependence of the dissociation. The observed spectra showed no difference for the different polarizations. However, the line widths of the nascent profiles were wide enough to measure the average translational energies of the OH fragments.

Results

A portion of the LIF spectra of the OH fragments produced from the photodissociation of acetic and trifluoroacetic acid at 193 nm is presented in Figure 2. In the spectra, individual rotational transitions in the 0−0 band of the A−X transition are resolved and assigned according to Dieke and Crosswhite.[12] For both molecules, the rotational transitions from the 1−1 band region have been measured, but no appreciable intensities exceeded the noise in the spectra. Thus, the population of OH in the higher vibrational states is negligible.

The rotational population distributions that peak at $N = 2$, 3 and extend to $N = 12$ were obtained from the measured spectra using the reported Einstein B coefficients[13] (Figure 3). The distributions are well represented by a Boltzmann distribution with temperatures of 1000 and 900 K for acetic acid and trifluoroacetic acid, which correspond to average rotational energies of the OH fragments of 695 and 625 cm^{-1}, respectively. In Figures 4 and 5, measured Λ-doublet and F1/F2 distributions are shown, which reveal statistical distributions in all cases.

To observe any polarization dependence in the dissociation, various rotational transitions were probed under different pump−probe geometries. The observed Doppler profiles were all Gaussian-like, implying no polarization dependence. However, the profiles were wide enough compared to our laser bandwidth

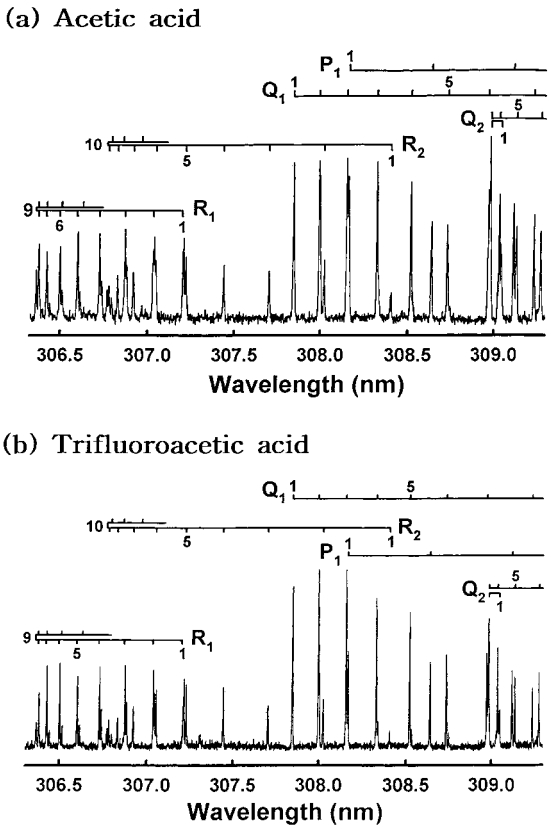

Figure 2. Portions of the LIF excitation spectra of OH produced from the photodissociation of acetic acid and trifluoroacetic acid at 193 nm employing the 0−0, A←X transition. The assignments are from ref 12.

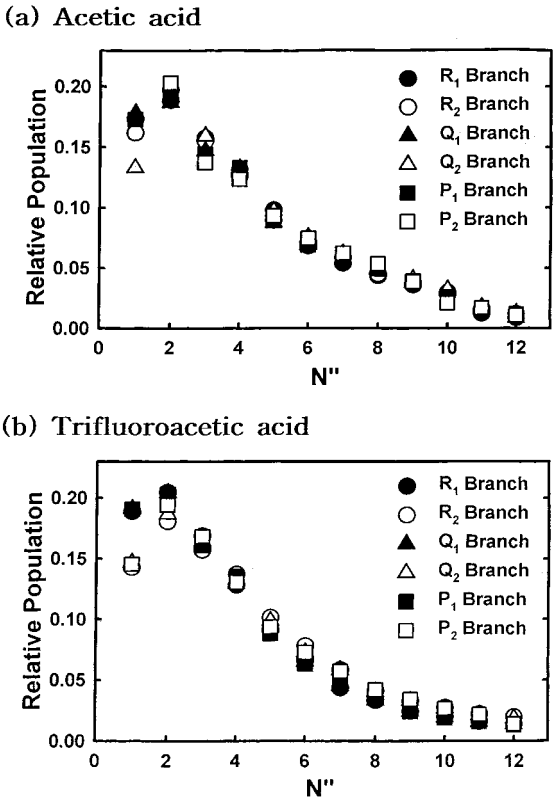

Figure 3. Rotational population distributions of OH obtained from the LIF spectra in Figure 2.

to measure the translational energy releases from the second moments of the profiles. Typical spectra are shown in Figure 6. The line widths of the measured profiles were slightly larger for low N and slightly smaller for high N than that measured for $N = 6$. The second moments were measured from the spectra

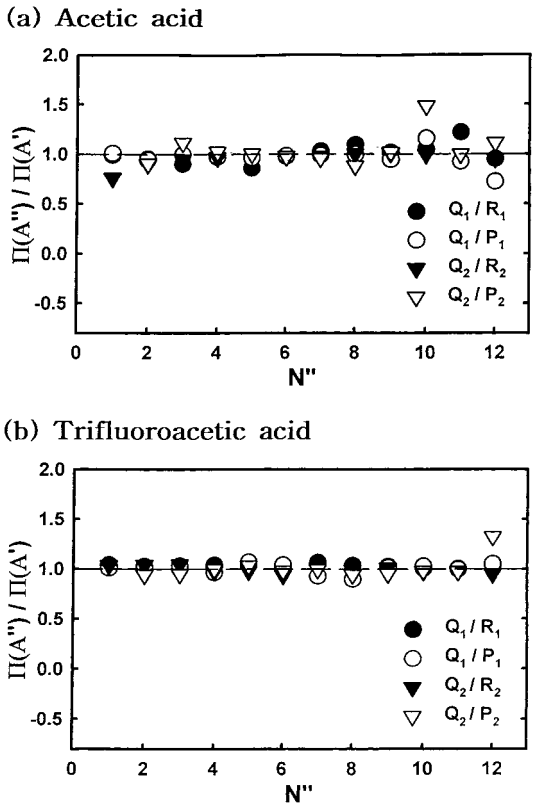

Figure 4. Measured F_1/F_2 ratios of OH produced from the photodissociation of acetic acid and trifluoroacetic acid at 193 nm.

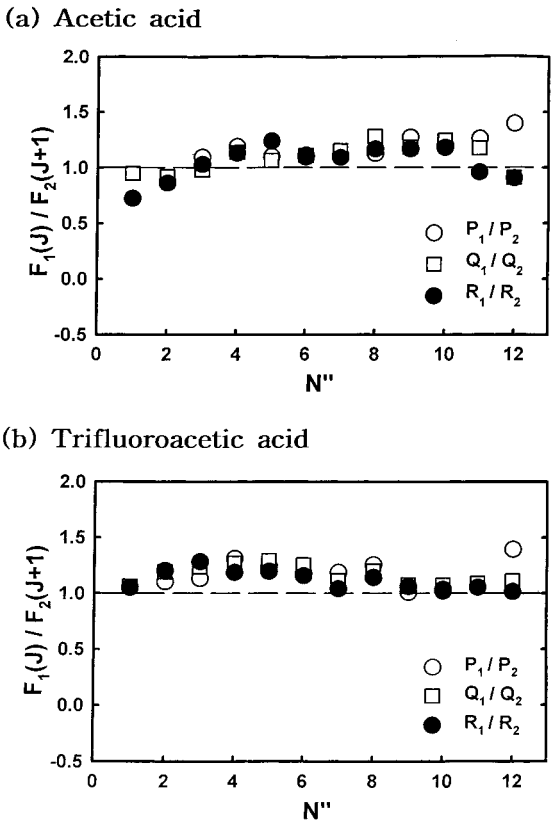

Figure 5. Measured Λ-doublet distributions OH produced from the photodissociation of acetic acid and trifluoroacetic acid at 193 nm.

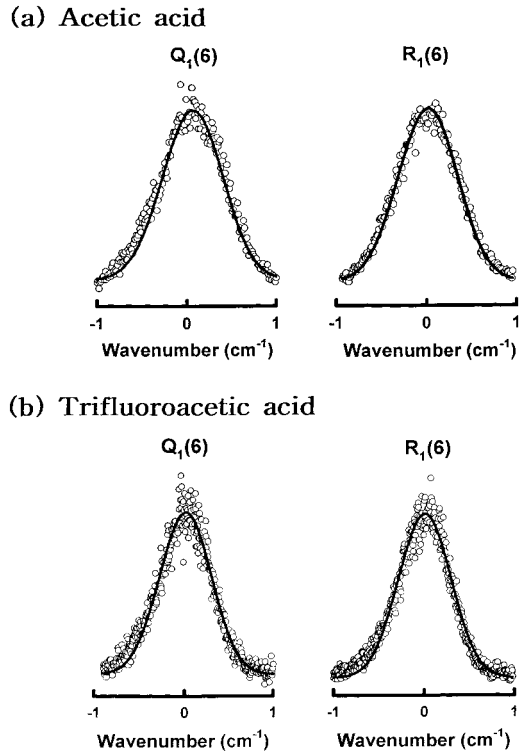

Figure 6. Rotationally resolved Doppler profiles of OH produced from the photodissociation of acetic and trifluoroacetic acid at 193 nm for different rotational branch transitions. The solid lines are simulations from the convolution of Gaussian line shape with laser bandwidth measured in Figure 1.

after deconvolution of the laser line width. The measured average translational energy releases in the center of mass system are 5890 and 4550 cm^{-1} for acetic acid and trifluoroacetic acid, respectively.

The available energy distributed among the fragments is then calculated from the photon energy (51800 cm^{-1}) and the internal energy of the parent molecule at room temperature (600 cm^{-1}) minus the dissociation energy. The dissociation energy of OH from trifluoroacetic acid has not been reported so far. Thus, the heat of formations of trifluoroacetic acid and trifluoroacetyl radical were obtained by ab initio calculation using the 6-311+G basis at the MP2 level using the GAUSSIAN 98 program package.[14] The calculated dissociation energies are 110 and 112 kcal/mol for acetic acid and trifluoroacetic acid, respectively. Since the dissociation energy of the acetic acid was obtained within ±2 kcal/mol of the value from the literature,[7] the calculated dissociation energy of trifluoroacetic acid is of similar accuracy at the present level of calculation. The complete energy partitioning among the product degrees of freedom was then obtained and listed in Table 1. In the table, the energy partitioning is also listed assuming, impulsive dissociation.[15] In this calculation, the geometry at the impulse is assumed to be the same for the COOH moiety as for the equilibrium geometry in the ground state obtained from geometry optimization by the above ab initio calculations. It is noted in the table that the translational energies are much smaller than those from the impulsive model calculations for both molecules.

Discussion

The absorption spectra of acetic acid and trifluoroacetic acid in the 40 000 ~ 70 000 cm^{-1} region show four bands, which are assigned as $n \rightarrow \pi^*$, $n \rightarrow$ 3s Rydberg, $\pi \rightarrow \pi^*$, and $n \rightarrow$ 3p Rydberg transitions, respectively.[16,17] In the ground electronic state, the C−(C═O)−O atoms are all in the plane, whereas the methyl group is predicted to be out-of-plane by molecular orbital interactions as a result of the lowest transition that leads the parent molecule to the $\pi^*_{C=O}$ singlet MO state.[18] However, the dissociation of OH by α-cleavage forming radical products has been known to take place along the triplet surface.[19] Thus, a curve crossing between the singlet and triplet surfaces is expected in the excited electronic states to produce primary photochemical products. This curve crossing is in general experimentally and theoretically observed in most of the carbonyl compounds such as acetone,[2] acetaldehyde,[20] and so forth.

TABLE 1: Fraction of the Available Energy Distributed among the Products Produced from the Photodissociation of Acetic Acid and Trifluoroacetic Acid at 193 nm

$E_{av}(cm^{-1})$	$\langle f_t \rangle$	$\langle f_r(OH) \rangle$	$\langle f_v(OH) \rangle$	$\langle f_{int}(acetyl) \rangle$
acetic acid				
14 000[a]	0.42	0.05	<0.01[b]	0.53[d]
impulsive model	0.56	0.03	0.001	
trifluoroacetic acid				
13 700[c]	0.33	0.05	<0.01[b]	0.62[d]
impulsive model	0.47	0.03	0.001	

[a] $E_{av} = h\nu(193\ nm) + E_{int}(CH_3COOH\ at\ 300\ K) - D_0(CH_3CO-OH)$. [b] Approximated from the noise in the spectra. [c] Obtained from the ab initio calculation. [d] Corresponding internal energies are 21.2 and 24.4 kcal/mol for acetyl and trifluoroactyl radicals, respectively.

In formic acid, for example, the curve crossing between the singlet and triplet surfaces exhibits a reverse barrier in the exit channel of the dissociation of OH.[21,22] The energy of the reverse barrier is transformed into translational energies of the products, which is manifested by the relative invariance of the translational energies of the products photodissociated at different excitation energies. The same should happen in the dissociation of acetic acid and trifluoroacetic acid in the present case. Recently, Guest and co-workers measured the translational energy of OH from the dissociation of acetic acid at 218 and 200 nm.[7,8] They measured 9.8 and 10.4 kcal/mol of translational energies of OH from the 218 and 200 nm dissociation, respectively, from which they suggested the reverse barrier of 13 kcal/mol for the OH production channel. If there were no exit channel barrier, the translational energy might have been expected to increase substantially with increasing photon energy. In the present study, the measured translational energy of OH from acetic acid at 193 nm is 12 kcal/mol, which is not much higher than those from the dissociation at lower excitation energies, considering the higher photon energy. The center of mass translational energy of the products from acetic acid photodissociation is 16.8 kcal/mol, which is the energy of the reverse barrier plus the statistical partitioning of the remaining available energy into translation.

In a diatomic molecule with a singly occupied p_π orbital such as OH produced in this experiment, coupling between the electronic angular momentum and nuclear rotation splits the two degenerate states of $\Lambda = \pm 1$, the orbital angular momentum projection to the internuclear axis.[23] In the limit of high rotation, the p_π orbital is approximated as a lobe aligned perpendicular to the plane of rotation (Π^-, the lower Λ state) or a lobe in the plane of rotation (Π^+, the upper Λ state). According to the parity selection rule, the Q-branch rotational transition is induced from the Π^- state, whereas the R- and P-branches transition from the Π^+ state in the electronic transition. Thus, the specific Λ-doublet population can be measured experimentally in the spectra. The distribution between the two Λ-doublet states of OH produced in the photodissociation depends on the correlation on the p_π orbital of the OH fragment with the orbitals of the

parent molecule and how the p_π orbital is generated upon dissociation, that is, the mechanism of the dissociation process. In other words, OH rotating in the plane containing the dissociating O−O bond axis as a result of in-plane dissociation would be expected provided the rotation of OH originates solely from the impulse upon dissociation, whereas out-of-plane dissociation would be expected if the parent torsional motion plays a role upon dissociation. The measured Λ-doublet distribution in this experiment shows no propensity in the two Λ-doublet states, implying that both the impulse and the parent torsion should be transformed into product rotational motion.

A recent photodissociation study of acetic acid at 194.5 nm using the femtosecond pump−probe technique showed the lifetime of the acetyl radical to be 5 ps.[11] The lifetime was successfully estimated by the RRKM theory assuming the internal energy of the acetyl radical from the previous 200 and 218 nm photolysis experiments. The average internal energy of 21.2 kcal/mol measured in this study should provide better estimates for the lifetime of the unimolecular acetyl radical dissociation. The calculated lifetime of the acetyl radical by the RRKM theory is 9.1 ps, which is a little overestimated. However, as Baronavski noted, one should not use average energy but rather internal energy distribution in the calculation to obtain a better result. Since we measured the rotational energy distribution of OH, we calculated the lifetime of the acetyl radical using the internal energy distribution that corresponds to the measured rotational distribution of OH in Figure 3. The calculated lifetime is 4.1 ps, which is in excellent agreement with the measured lifetime by Baronavski. In trifluoroacetic acid, the fluorine substitution substantially weakens the C−C bond, resulting in a dissociation energy of 7.8 kcal/mol compared to 17.6 kcal/mol for acetic acid. The measured average internal energy is 24.3 kcal/mol in the trifluoroacetyl radical, from which the lifetime is calculated to be 0.63 ps by the RRKM calculations. Though the internal energy of the trifluoroacetyl radical is not much higher than that of the acetyl radical, the dissociation rate is about 7 times faster because the E/Ec is about 3 times larger.

In this study, the photodissociation dynamics of the acetic acid and trifluoroacetic acid have been investigated and the average internal energies of the acetyl and trifluoroacetyl radicals have been measured. The dissociation takes place indirectly along the triplet surface via curve crossing with the reverse barrier in the exit channel. From the measured average internal energies, the average lifetimes have been estimated to be 4.3 and 0.63 ps for the acetyl and trifluoroacetyl radicals, respectively, by the RRKM theory.

Acknowledgment. This work has been financially supported by the Korea Science and Engineering Foundation.

References and Notes

(1) Calvert, J. G.; Horowits, A. *J. Phys. Chem.* **1982**, *86*, 3105.

(2) Trentelman, K. A.; Kable, S. H.; Moss, D. B.; Houston, P. L. *J. Chem. Phys.* **1989**, *91*, 7498.

(3) North, S. W.; Marr, A. J.; Furlan, A.; Hall, G. E. *J. Phys. Chem. A* **1997**, *101*, 9224.

(4) Maul, C.; Haas, T.; Gericke, K.-H. *J. Phys. Chem. A* **1997**, *101*, 6619.

(5) Kim, S. K.; Pedersen, S.; Zewail, A. *J. Chem. Phys*. **1995**, *103*, 477.

(6) Singleton, D. L.; Paraskevopoulos, G.; Irwin, R. S. *J. Phys. Chem.* **1990**, *94*, 695.

(7) Hunnicutt, S. S.; Waits, L. D.; Guest, J. A. *J. Phys. Chem.* **1989**, *93*, 5188.

(8) Hunnicutt, S. S.; Waits, L. D.; Guest, J. A. *J. Phys. Chem.* **1991**, *95*, 562.

(9) Peterman, D. R.; Daniel, R. G.; Horwitz, R. J.; Guest, J. A. *Chem. Phys. Lett*. **1995**, *236*, 564.

(10) North, S. W.; Blank, D. A.; Gezelter, J. D.; Longfellow, C. A.; Lee, Y. T. *J. Chem. Phys.* **1995**, *102*, 4447.

(11) Owrutsky, J. C.; Baronavski, A. P. *J. Chem. Phys.* **1999**, *111*, 7329.

(12) Dieke, G. H.; Crosswhite, H. M. *J. Quant. Spectrosc. Radiat. Transfer* **1962**, *2*, 97.

(13) Chidsey, I. L.; Crosely, D. R. *J. Quant. Spectrosc. Radiat. Transfer* **1980**, *23*, 187.

(14) Gaussian 98, Frisch, M. J.; Trucks, G. W.; Schlegel, H. B.; Scuseria, G. E.; Robb, M. A.; Cheeseman, J. R.; Zakrzewski, V. G.; Montgomery, J. A.; Stratmann, R. E.; Burant, J. C.; Dapprich, S.; Millam, J. M.; Daniels, A. D.; Kudin, K. N.; Strain, M. C.; Farkas, O.; Tomasi, J.; Barone, V.; Cossi, M.; Cammi, R.; Mennucci, B.; Pomelli, C.; Adamo, C.; Clifford, S.; Ochterski, J.; Perdersen, G. A.; Ayala, P. Y.; Cui, Q.; Morokuma, K.; Malick, D. K.; Rabuck, A. D.; Raghavachari, K.; Foresman, J. B.; Cioslowski, J.; Ortiz, J. V.; Stefanov, B. B.; Liu, G.; Liashenko, A.; Piskorz, P.; Komaromi, I.; Gomperts, R.; Martin, R. L.; Fox, D. J.; Keith, T.; Al-Laham, M. A.; Peng, C. Y.; Nagayakkara, A.; Gonzales, C,; Challacombe, M.; Gill, P. M. W.; Johnson, B. G.; Chen. W.; Wong, M. W.; Andres, J. L.; Head-Gordon, M.; Replogle, E. S.; Pople, J. A. Gaussian Inc.: Pittsburgh, PA, 1998.

(15) Tuck, A. F. *J. Chem. Soc., Faraday Trans. 2*, **1977**, *73*, 689.

(16) Basch, H.; Robin, M. B.; Kuebler, N. A. *J. Chem. Phys.* **1968**, *49*, 5007.

(17) Barnes, E. E.; Simpson, W. T. *J. Chem. Phys.* **1963**, *39*, 670.

(18) Walsh, A. D. *J. Chem. Soc. (London)* **1953**, 1953, 2306.

(19) Yadav, J. S.; Goddard, J. D. *J. Chem. Phys.* **1986**, *84*, 2682.

(20) Kono, T.; Takayanagi, M.; Hanazaki, I. *J. Phys. Chem.* **1993**, *97*, 12793.

(21) Brouard, M.; Simons, J. P.; Wang, J. X. *Faraday Discuss. Chem. Soc.* **1991**, *91*, 63.

(22) Shin, S. K.; Han, E. J.; Kim, H. L. *J. Photochem. Photobiol. A* **1998**, *118*, 71.

(23) Andresen, P.; Rothe, E. W. *J. Chem. Phys.* **1985**, *82*, 3634.